Analyzing DEM simulations with two different contact models: Cundall-Strack and Hertz-Mindlin model

Rahul Pandare | May 25, 2025

Overview of key differences between the two contact models - Cundall-Strack (CS) and Hertz-Mindlin (HM) model

1 Introduction & Motivation

The Discrete Element Method (DEM) is a widely used computational technique for modeling the behavior of granular materials. It provides a framework for solving the governing equations of motion for systems of interacting particles under specified conditions. In the literature, two contact models are frequently employed in DEM simulations: the Cundall-Strack (CS) model and the Hertz-Mindlin (HM) model [1, 4, 5]. Understanding the differences between these models is essential for selecting the appropriate one for a given application. These differences manifest in several physical and computational aspects, including the system's kinetic energy, particle overlaps (reflecting material stiffness), tangential force distributions, and velocity profiles. This study aims to explore and compare the CS and HM models in detail, providing insights into their behavior through quantitative and visual analyses.

2 System & Models

Before implementing the contact models, we require a base DEM simulation framework upon which these models can be integrated. I provide a step-by-step guide for building such a DEM simulation in a separate article, available here. In this study, I consider a two-dimensional system composed of polydisperse circular discs. The system is relatively dense, with a packing fraction of $\phi = 0.50$, meaning that particles occupy 50% of the simulation box area. The domain features periodic boundaries, and gravitational forces are neglected. Particles are assumed to be nearly rigid. To ensure sufficient statistical reliability, the system contains 100 particles. The interparticle friction coefficient is set to $\mu = 0.7$. The initial configuration is generated using a random packing algorithm that minimizes particle overlaps, thereby preventing the onset of large, non-physical forces at the beginning of the simulation. Only one type of interaction is considered: pairwise contact interactions between particles. These are modeled using either the Cundall-Strack or Hertz-Mindlin model, and the results from both approaches are compared in this article.

2.1 Cundall-Strack Model

Developed by P.A. Cundall and O.D.L. Strack in 1979, this model remains one of the most popular contact models used in discrete element method (DEM) simulations [2]. It is a linear contact model that calculates contact forces based on particle overlaps, using relatively simple routines to compute the normal and tangential forces between interacting particles.

The CS model represents the contact forces as a combination of linear springs and dashpots, modeling both elastic and damping effects in the normal and tangential directions:

$$\mathbf{F}_n = \underbrace{-k_n \delta_n \mathbf{n}}_{\text{elastic}} - \underbrace{\gamma_n \mathbf{v}_n^{ij}}_{\text{damping}} \tag{1}$$

$$\mathbf{F}_t = \underbrace{-k_t \boldsymbol{\xi}_t}_{\text{elastic}} - \underbrace{\gamma_t \mathbf{v}_t^{ij}}_{\text{damping}} \tag{2}$$

where

- $\mathbf{F}_n$, $\mathbf{F}_t$ are the normal and tangential contact forces,
- k_n, k_t are the normal and tangential stiffness constants,
- δ_n, $\boldsymbol{\xi}_t$ are the normal and tangential displacements (overlaps),
- $\mathbf{v}_n^{ij}$, $\mathbf{v}_t^{ij}$ are the relative normal and tangential velocities between the interacting particles.

The tangential spring displacement $\boldsymbol{\xi}_t$ is initialized as zero at the start of every potential contact. Therefore, it is important to begin the simulation with negligible overlaps to avoid nonphysical forces. During contact, $\boldsymbol{\xi}_t$ is updated and stored throughout the duration of the contact, and reset to zero once the contact is lost:

$$\boldsymbol{\xi}_t^{\text{new}} = \begin{cases} \boldsymbol{\xi}_t^{\text{old}} + \mathbf{v}_t^{ij} \Delta t, & \delta_n > 0 \\ 0, & \delta_n \leq 0 \end{cases}$$

Here, Δt is the simulation time-step.

The normal displacement is calculated geometrically as:

$$\delta_n = (a_i + a_j) - (\mathbf{r}_i - \mathbf{r}_j) \cdot \mathbf{n}$$

where a_i, a_j are the radii and $\mathbf{r}_i, \mathbf{r}_j$ are the position vectors of the interacting particles.

The CS model is often referred to as a stick-slip model because it enforces the Coulomb friction limit on the tangential force:

$$|\mathbf{F}_t| \leq \mu |\mathbf{F}_n|$$

If this limit is exceeded, both the tangential force and displacement are scaled back to the maximum allowable values, ensuring that the contact transitions from sticking to sliding:

$$|\mathbf{F}_t^{\max}| = \mu|\mathbf{F}_n| \tag{3}$$

$$\boldsymbol{\xi}_t^{\max} = \boldsymbol{\xi}_t \cdot \frac{|\mathbf{F}_t^{\max}|}{|\mathbf{F}_t|} \tag{4}$$

The linear spring-dashpot system can be interpreted as a damped harmonic oscillator with normal damping coefficient γ_n and characteristic contact time t_c given by:

$$\gamma_n = 2\eta\sqrt{m_{ij}k_n}$$

$$t_c = \frac{\pi}{\omega}, \quad \text{where} \quad \omega = \sqrt{\frac{k_n}{m_{ij}} - \left(\frac{\gamma_n}{2m_{ij}}\right)^2}$$

$$m_{ij} = \frac{m_i m_j}{m_i + m_j}$$

Here, η is the damping ratio (commonly chosen as $\eta = 0.3$) and m_{ij} is the reduced mass of the interacting pair.

For simulations of very rigid particles, the stiffness dominates over damping ($k_n \gg \gamma_n$), allowing us to approximate the contact time as:

$$t_c \approx \sqrt{\frac{m_{ij}}{k_n}}$$

To ensure numerical stability and accurate resolution of the contact dynamics, the simulation time-step must satisfy:

$$\Delta t \ll t_c$$

This prevents unrealistically large overlaps and forces that could destabilize the simulation.

The tangential stiffness and damping coefficients are typically chosen proportional to their normal counterparts; here, we set:

$$k_t = \frac{1}{2}k_n, \quad \gamma_t = \frac{1}{2}\gamma_n$$

2.2 Hertz-Mindlin Contact Model

The theory of frictional elasticity for contacting spheres was first developed by Hertz in 1882, modeling only the normal contact force [3]. However, Hertz's model did not account for tangential forces that occur during oblique particle contacts. Later, Mindlin and Deresiewicz extended this theory to include tangential forces, developing a nonlinear contact model that better represents the physical mechanics of real contacts [6].

The normal contact force in the Hertzian model is given by:

$$\mathbf{F}_n = \frac{4}{3}E_{\text{eff}}\sqrt{R_{\text{eff}}}\,\delta_n^{3/2}\,(1 + f_d),$$

where the effective radius is defined as

$$R_{\text{eff}} = \frac{a_i a_j}{a_i + a_j}.$$

The normal displacement and damping fraction are:

$$\delta_n = \min(0, \delta_n^{\max}),$$

$$f_d = \max\left(0, -\eta_n \, \mathbf{v}_n^{ij}\right),$$

where η_n is the normal damping coefficient, $\mathbf{v}_n^{ij}$ is the relative normal velocity between particles, and $\delta_n^{\max}$ is the maximum allowable overlap, set to 0.01 to reflect the rigidity of the particles.

The tangential force follows the same formulation as in the Cundall-Strack model (Eq. 2) and obeys Coulomb's friction law, with the rescaling of tangential force and displacement as described in Eqs. 3 and 4.

Material parameters used in the simulation include Young's modulus $E = 7 \times 10^{10}$ Pa (typical for silica particles) and Poisson's ratio $\nu = 0.3$. The derived mechanical parameters are summarized below:

Parameter	**Expression**
Shear modulus	$G = \dfrac{E}{2(1+\nu)}$
Effective Young's modulus	$E_{\text{eff}} = \dfrac{E}{1-\nu^2}$
Tangential stiffness constant	$k_t = 8G\sqrt{R_{\text{eff}}\,\delta_n}$
Effective radius	$R_{\text{eff}} = \dfrac{a_i a_j}{a_i + a_j}$
Effective mass	$m_{\text{eff}} = \dfrac{m_i m_j}{m_i + m_j}$

Table 1: Mechanical parameters used in the Hertz-Mindlin contact model.

3 Results

The primary parameters compared between the two contact models are the normal and tangential forces, the normal displacement (overlap), and the kinetic energy of interacting particles.

Figure 1 shows that, in the Cundall-Strack (CS) model, the contact forces tend to decay over time, whereas in the Hertz-Mindlin (HM) model, the forces remain more consistently distributed throughout the simulation. Although damping is present in both models, the characteristic time scales differ significantly due to the much higher elastic stiffness in the

HM model, which employs a very large Young's modulus ($E \sim \mathcal{O}(10^9)$ Pa) to represent stiff particles. It is likely that, over longer simulation times, the force distribution in the HM model would also decay similarly to the CS model.

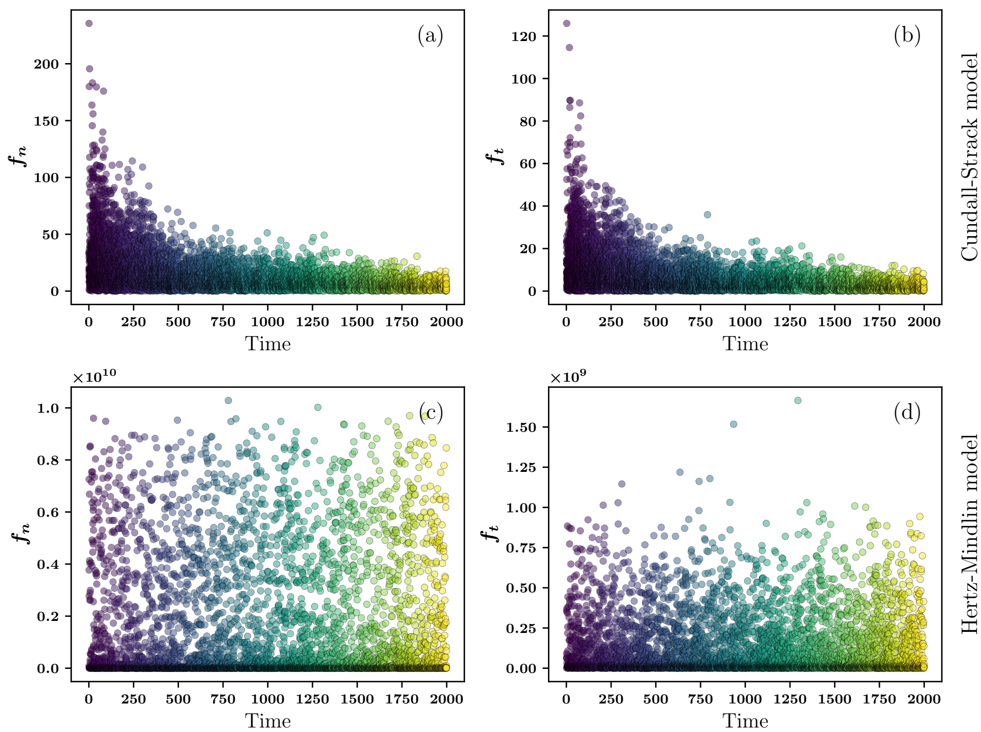

Figure 1: Time evolution of normal and tangential forces for both models. Panels (a) and (b) show the normal and tangential forces, respectively, for the Cundall-Strack model, while panels (c) and (d) show the corresponding forces for the Hertz-Mindlin model.

Figure 2 presents the maximum normal displacement (overlap) observed at each time step. The normal displacement δ_n decreases over time in the CS model, reflecting the decay of contact forces. In contrast, δ_n remains approximately constant in the HM model, likely due to its higher force resolution. In both models, the overlap remains below 1%, confirming that the particles behave as effectively rigid bodies—a design goal of the simulation. This also serves as a secondary validation of the simulation's physical consistency.

Figure 3 illustrates the kinetic energy of only the interacting particles, excluding those not in contact to focus on the dynamics of particle collisions and contacts. Consistent with the force data, the kinetic energy in the CS model decreases over time, indicating energy dissipation. Conversely, the kinetic energy in the Hertz-Mindlin (HM) model remains approximately constant throughout the simulation. This behavior is clearly illustrated in the simulation movies of the Cundall-Strack (CS) model and the Hertz-Mindlin (HM) model, both available in the GitHub repository.

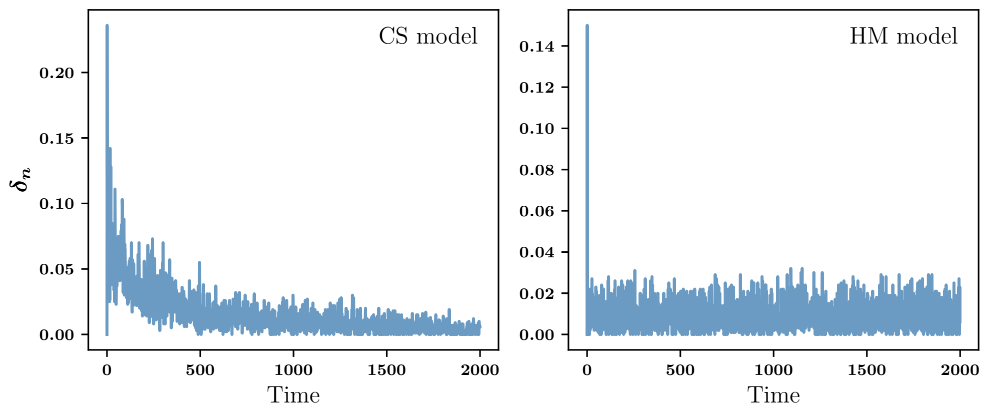

Figure 2: Maximum normal displacement (overlap) for all particle interactions over time in (a) the Cundall-Strack model and (b) the Hertz-Mindlin model.

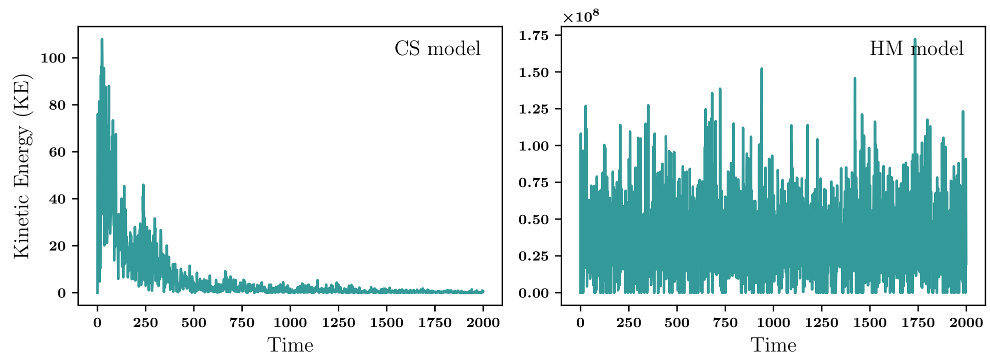

Figure 3: Kinetic energy of interacting particles over time in (a) the Cundall-Strack model and (b) the Hertz-Mindlin model.

4 Summary

In this article, we compared key parameters of two contact models—Cundall-Strack (CS) and Hertz-Mindlin (HM)—using the same physical system but different numerical approaches to resolving particle contacts. The CS model is simpler and computationally efficient, requiring less stringent time resolution, making it a practical tool for studying the time evolution of granular systems while providing reasonable estimates of contact forces. In contrast, the HM model is more complex and computationally intensive, offering higher accuracy in force predictions that align better with experimental results [4]. However, its high computational cost makes it less suitable for long-time dynamic simulations. For overdamped systems such as LF-DEM[5], where simulations are typically run up to a target strain and the distribution of forces is more important than absolute accuracy, the CS model provides a justified and faster alternative without significant loss of physical insight.

5 Resources

All codes, interaction data files, and simulation animations used in this study are publicly available on GitHub: github.com/rahul-pandare/DEM_simulations

References

[1] Jérôme Crassous. Discrete-element-method model for frictional fibers. *Physical Review E*, 107(2):025003, 2023.

[2] Peter A Cundall and Otto DL Strack. A discrete numerical model for granular assemblies. *geotechnique*, 29(1):47–65, 1979.

[3] Heinrich Hertz. Über die berührung fester elastischer körper. *J reine und angewandte Mathematik*, 92:156, 1881.

[4] Cheng Hu, Jingwei Gao, Jincheng Diao, and Xiaobo Song. Numerical simulation of tire steering on sandy soil based on discrete element method. *AIP Advances*, 11(1), 2021.

[5] Romain Mari, Ryohei Seto, Jeffrey F Morris, and Morton M Denn. Shear thickening, frictionless and frictional rheologies in non-brownian suspensions. *Journal of Rheology*, 58(6):1693–1724, 2014.

[6] Raymond D Mindlin and HERBERT Deresiewicz. Elastic spheres in contact under varying oblique forces. 1953.